

state ($\tau_{1/2} \leq 10^{-9}$ sec). The levels at 297 and 362 keV have been given their assigned spin and parity assignments as a result of Coulomb excitation experiments.¹⁴

The levels at 538 and 650 keV in Rh¹⁰³ have been established in energy by coincidence experiments.^{8,13} The 610-keV gamma ray has a measured *K*-shell conversion coefficient⁶ of 6×10^{-4} so that the transition may be regarded as *E1*. The parity of the 650-keV level is thus negative. Since the 557-keV gamma ray is of an intensity differing by less than one order of magnitude from that of the 610-keV gamma ray, it too may be considered to be *E1*, essentially ruling out the possibility that the 650-keV level have spin and parity $\frac{5}{2}^-$.

The analysis of (*d,p*) stripping reactions²² yields $\frac{5}{2}^+$

for spin and parity of the ground state of Ru¹⁰³. Values of *logft* for the beta spectra terminating at the energy states at 650 and 538 keV are 5.7 and 5.6, respectively.¹³ Consistent with these values of *logft* are spin-parity assignments of $\frac{7}{2}^-$ and $\frac{5}{2}^+$ for the 650- and 538-keV states. Additional evidence for assignment of positive parity to the 538-keV level is found in the fact that the *K*-shell conversion coefficient^{2,7,10} of the 498-keV gamma ray suggests it to be *M1* or *E2*. That spin and parity of the 538-keV level are $\frac{5}{2}^+$ rather than $\frac{7}{2}^+$ is supported by the fact that the 498-keV gamma ray and the 445-keV gamma ray differ so greatly in relative intensity, suggesting that these transitions do proceed according to different sets of selection rules.

Proton Spectra from Reactions Induced by 30.5-MeV Alpha Particles*

L. W. SWENSON†

*Department of Physics and Laboratory for Nuclear Science, Massachusetts Institute of Technology,
Cambridge, Massachusetts*

and

Bartol Research Foundation of The Franklin Institute, Swarthmore, Pennsylvania

AND

C. R. GRUHN‡

*Department of Physics and Laboratory for Nuclear Science, Massachusetts Institute of Technology,
Cambridge, Massachusetts*

(Received 3 December 1965; revised manuscript received 16 February 1966)

The (α,p) reaction has been studied at 30.5 MeV for the targets Al²⁷, Ti⁴⁸, V⁵¹, Fe, Co⁵⁹, Ni⁵⁸, Ni⁶⁰, Ni⁶¹, Ni⁶², Cu⁶³, Cu⁶⁵, Zn⁶⁷, Nb⁹³, Mo, Rh¹⁰³, Pd, Cd¹¹³, Cd¹¹⁴, Sn¹¹⁹, Sn¹²⁰, Sn¹²⁴, Ta¹⁸¹, Pt¹⁹⁵, and Au¹⁹⁷. Proton evaporation spectra were measured at 30, 60, 90, 120, and 150° up to excitation energies of 25 MeV in the residual nucleus. The spectra have been compared with statistical-model predictions and the parameters *a* and *T* obtained. The lack of mass dependence of these parameters and the average low value of the level-density parameter $a = 5.5 \text{ MeV}^{-1}$ add evidence for a nuclear-temperature anomaly. The anomaly is discussed in terms of recent intermediate-resonance models.

1. INTRODUCTION

THE statistical model is supported by a large body of experimental information accumulated over the past decade. The model has been widely applied to nuclear-reaction studies involving medium-energy neutrons, protons, alpha particles and to some extent He³, deuterons and heavy ions as bombarding particles on intermediate and heavy nuclei ($A > 25$). A comprehensive review of the existing experimental support for the statistical model has been given by Bodansky.¹ That a wide range of measurements of yields, level

spacings and emission spectra can be successfully accounted for in terms of the nuclear level density is the most compelling evidence in support of the statistical model.

An understanding of the magnitude of the level density and its dependence upon excitation energy and mass is central to the successful application of the statistical model. The dependence of the level density on excitation energy and mass is influenced by the details of the assumed nuclear model and is parametrized by the nuclear-temperature or Fermi-gas-model level-density parameter *a*. The excitation-energy dependence of the level-density parameter has been the subject of numerous investigations of which the presently reported study is an additional example.

A comprehensive survey of the mass dependence of the parameter *a* have been made by Lang² and Erba,

* This work was supported in part by funds provided by the U. S. Atomic Energy Commission under Contract No. AT(30-1)-2098, and the National Science Foundation.

† Present address: Bartol Research Foundation, Swarthmore, Pennsylvania.

‡ Present address: Department of Physics, Michigan State University, East Lansing, Michigan.

¹ D. Bodansky, *Ann. Rev. Nucl. Sci.* **12**, 79 (1962).

² D. W. Lang, *Nucl. Phys.* **26**, 434 (1961).

Facchini, and Menichella³ for neutron and proton-induced reactions at medium energies. Lang has compared the observed dependence of a on A with predictions of Newton's⁴ shell-model level-density formula, and found very satisfactory agreement. The agreement is particularly significant since the experimental a values were derived from a wide range of experimental sources such as direct counting of neutron resonances near the neutron binding energy, excitation-function experiments and analysis of spectra from (n,n') , (n,p) , (p,n) , and (p,p') -reaction studies initiated by particles of different bombarding energies. Several investigators^{5,6} have also reported good agreement between temperatures derived from (p,p') spectra and from direct level counting of low-lying levels in a number of medium-weight nuclei.

The question of the mass dependence of a for alpha-particle-induced reactions is less well resolved. In previous evaluations of a from (α,p) and (α,α') spectra, the level density parameter has shown a marked dependence on bombarding energy; further, the available data⁷⁻¹³ were sufficiently incomplete to prevent a meaningful comparison with the shell-dependent predictions of Newton. The study initiated in Ref. 1 has been extended to a wider range of nuclei and the experimental technique has been improved to permit the study of alpha-particle-induced reactions at higher excitation energies.

The experimental results reported in the sections that follow have been compared to specific statistical-model predictions and add further evidence of a nuclear-temperature anomaly for alpha-particle-induced reactions. The a values from the (α,p) reaction at 30.5 MeV are essentially mass-independent with an average value of 5.5 MeV^{-1} for the mass region $A=30-200$. They show no prominent shell structure. Finally, the possible cause of the anomaly is discussed in terms of recent intermediate-resonance models.¹⁴⁻¹⁷

2. EXPERIMENT

The significant physical quantity measured was the proton energy spectrum from the (α,p) reaction at

³ E. Erba, U. Facchini, and E. S. Menichella, *Nuovo Cimento* **22**, 1237 (1961).

⁴ T. D. Newton, *Can. J. Phys.* **34**, 804 (1956).

⁵ N. M. Hintz and V. Meyer, *Bull. Am. Phys. Soc.* **6**, 441 (1961).

⁶ N. MacDonald and A. C. Douglas, *Nucl. Phys.* **24**, 614 (1961).

⁷ W. Swenson and N. Cindro, *Phys. Rev.* **123**, 910 (1961).

⁸ R. M. Eisberg, G. Igo, and H. E. Wegner, *Phys. Rev.* **100**, 1309 (1955).

⁹ N. O. Lassen and V. A. Siderov, *Nucl. Phys.* **19**, 579 (1960).

¹⁰ V. A. Siderov, *Nucl. Phys.* **35**, 253 (1962).

¹¹ R. Fox and R. D. Albert, *Phys. Rev.* **121**, 587 (1961).

¹² H. W. Fulbright, N. O. Lassen, and N. O. Roy Poulsen, *Kgl. Danske Videnskab. Selskab, Mat. Fys. Medd.* **31**, No. 19 (1959).

¹³ B. Pate (private communication).

¹⁴ K. Izumo, *Progr. Theoret. Phys. (Kyoto)* **26**, 807 (1961).

¹⁵ K. Izumo, *Nucl. Phys.* **62**, 673 (1965).

¹⁶ A. K. Kerman, L. S. Rodberg, and J. E. Young, *Phys. Rev. Letters* **11**, 422 (1963).

¹⁷ B. Block and H. Feshbach, *Ann. Phys. (N. Y.)* **23**, 47 (1963).

several laboratory angles. The experimental approach was to use an E - dE/dx counter telescope and pulse-multiplying circuit to effect particle identification and then to store the energy spectra of the emitted particles in the memory of a multichannel analyzer.

The reactions studied in the experiment were induced by alpha particles accelerated to 30.5 MeV by the MIT 42-in. cyclotron. The beam from the cyclotron after being focused by a pair of magnetic-quadrupole lenses entered a 5-in.-diam scattering chamber through beam-defining slits and was incident upon a target mounted at the center of the chamber as illustrated in Fig. 1. The beam then passed through the chamber into a lead-lined Faraday cup where the beam was integrated for monitoring the beam current. An E - dE/dx counter telescope was mounted at 30° , 60° , 90° , 120° , and 150° ports in the scattering-chamber wall.

The dE/dx counter consisted of an argon-methane-filled proportional counter of 6.35-cm active length and filled to one atmosphere pressure. The filling gas was allowed to circulate with a flow rate of about one cm^3 per minute. The entrance window was 0.00025-in. aluminized Mylar. The collecting electrode of the proportional counter was placed off center to allow the reaction particles to pass through and into the E counter where they were stopped. The E counter consisted of a cylindrically shaped CsI scintillator 0.35 in. in diameter and 0.18 in. thick mounted on the face of an RCA 6199 photomultiplier tube. The dE/dx -counter resolution for 7-MeV incident protons was 12% and the E -counter resolution 4%. As the chief interest in these experiments was in the gross features of the emission spectra, only moderate energy resolution was required.

In the present experiment protons in the 1.5- to

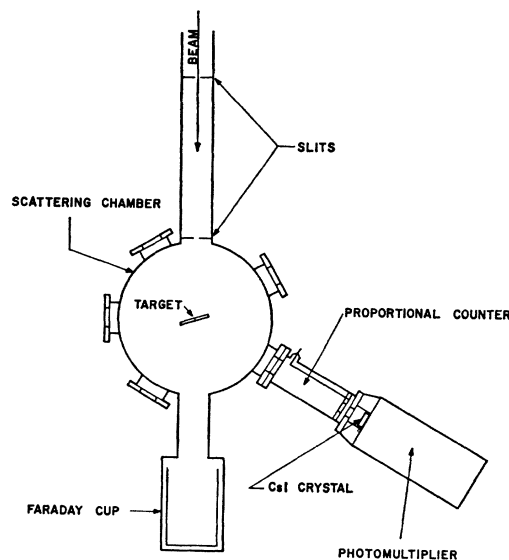


FIG. 1. Schematic representation of scattering chamber and detector assembly.

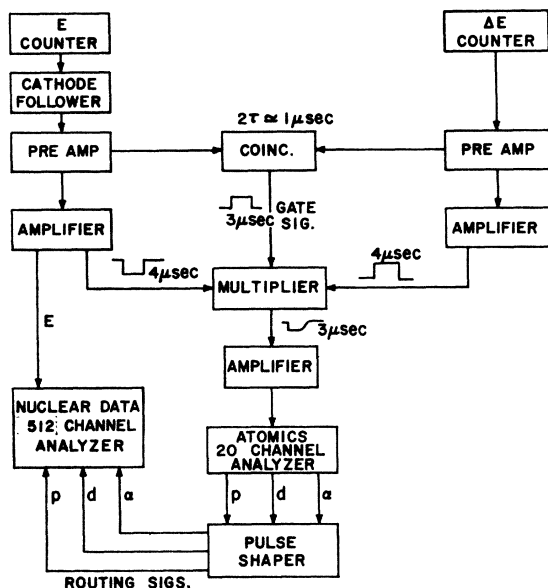


FIG. 2. Block diagram of electronic arrangement.

35-MeV range, deuterons in the 4- to 20-MeV range, and alpha particles in the 7- to 30-MeV range together with a small contribution from He^3 and tritons were detected and identified. The energy spectra of these particle types were accumulated in the memory of a Nuclear Data 512-channel analyzer. A block diagram of the electronic arrangement is shown in Fig. 2. The electronics used were for the most part conventional with the exception of the pulse-multiplying circuit.

The multiplying circuit used to obtain the $E \cdot dE/dx$ product was designed to have a broad energy range. To a first approximation the $E \cdot dE/dx$ product is proportional to MZ^2 and energy independent, where M is the mass of the particle passing through the telescope and Z its charge. The product is not strictly energy-independent, however, and care must be taken in the design of the multiplying circuit if different particle types are to be identified over a broad energy range. The multiplier circuit used in the experiment is described in detail elsewhere.¹⁸ The multiplier pulse-height spectrum was analyzed by an Atomic Instrument Company 20-channel analyzer. The analyzer was modified such that the scalar driver signals were summed for all channels within the pulse-height range corresponding to a given particle type, viz., protons, deuterons, or alpha particles. After pulse shaping, these signals served as routing pulses to the 512-channel analyzer. Thus the proton, deuteron and alpha particle energy spectra could each be stored in a different 128-channel quadrant of the 512-channel analyzer memory.

A typical $E \times \Delta E$ multiplier spectrum as it appeared in the 20-channel analyzer is shown in Fig. 3. The deuterons are shown to be clearly distinguished from the larger proton group. All pulses appearing above

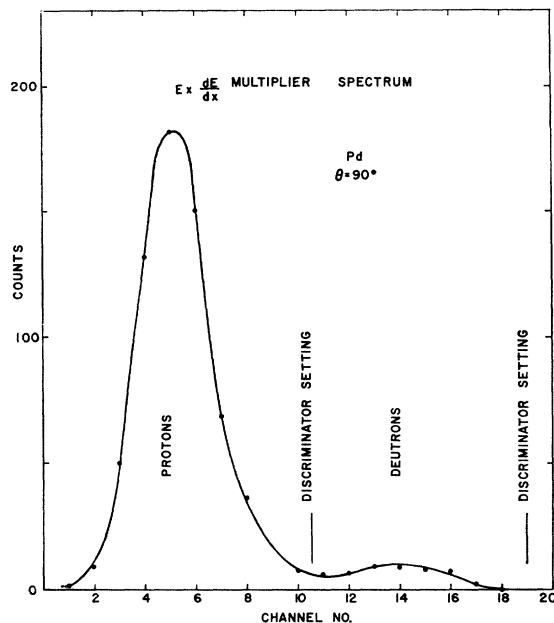


FIG. 3. The $E \times dE/dx$ multiplier spectrum for Pd at 90° is represented as a function of channel number of the Atomic Instrument Company 20-channel analyzer. All triton, alpha-particle, and He^3 events would appear above channel 19 and are present in the overflow channel. A continuous proton energy range of 1.5 to 30 MeV, deuteron range 3.5 to 16 MeV, and alpha-particle range of 7 to 30 MeV are represented by the above figure.

channel 20 (in the overflow channel) are treated as alpha particles, which would include any tritons or He^3 if present among the reaction products.

A coincidence, with $2\tau \approx 1 \mu\text{sec}$, is effected between the ΔE and E signals to prevent storage of neutron and gamma-ray events or pulses corresponding to charged particles which did not pass through both the E and ΔE sections of the telescope.

Energy spectra were calibrated by using reactions of known Q values. The proton-energy calibration was obtained using the reactions $\text{C}^{12}(\alpha, p)\text{N}^{15}$ $Q = -4.96$ MeV, $\text{C}^{12}(d, p)\text{C}^{13}$ $Q = 2.72$ MeV, and elastic scattering of protons and deuterons from gold. The incident proton, deuteron, and alpha-particle energies were 7.5, 15.0, and 30.5 MeV, respectively. The alpha-energy calibration was obtained using the elastic scattering of alpha particles from carbon and gold and the $\text{C}^{12}(\alpha, \alpha')$ $Q = -4.43$, -7.65 , and -9.6 MeV reactions.

Twenty-five targets: Al^{27} , Ti^{48} , V^{51} , Fe , Co^{59} , Ni^{58} , Ni^{60} , Ni^{61} , Ni^{62} , Cu^{63} , Cu^{65} , Zn^{67} , Zr , Nb^{93} , Mo , Rh^{103} , Pd , Cd^{113} , Cd^{114} , Sn^{119} , Sn^{120} , Sn^{124} , Ta^{181} , Pt^{195} , and Au^{197} in the 1 to 5 mg/cm^2 range were used in the experiment. All targets were self-supporting foils. Light-element contaminations such as carbon and oxygen were carefully avoided as they have large (α, p) cross sections.

3. DATA ANALYSIS

The testing ground of a compound-nucleus analysis of the experimental data is the comparison between the

¹⁸ L. W. Swenson, Nucl. Instr. Methods **31**, 269 (1964).

experimentally determined emission spectra and level-density parameters with those predicted by the statistical model. It will be seen that, analysis of the present experiment from the statistical-model point of view enjoys a good deal of success, but also offers evidence of contributing mechanisms other than the usual compound-nuclear process.

From statistical theory,¹⁹ the relative intensity of the particles emitted from the reaction $X(a,b)Y$ in the exit-channel energy range ϵ to $\epsilon+d\epsilon$ is represented by

$$N_b d\epsilon = \text{const} \sigma_c(\epsilon) \epsilon \omega(\epsilon_{\text{max}} - \epsilon) d\epsilon, \quad (1)$$

where $\sigma_c(\epsilon)$ is the capture cross section of the inverse reaction and $\omega(E)$ the density of states of the residual nucleus at the excitation energy $E = \epsilon_{\text{max}} - \epsilon$. The maximum channel energy ϵ_{max} corresponds to the residual nucleus being left in its ground state. The quantity N_b corresponds to the experimentally measured cross section $d^2\sigma/d\Omega dE$.

The inverse capture cross section is usually assumed to be equal to the total reaction cross section given by

$$\sigma_c = \pi \lambda^2 \sum_{l=0}^{\infty} (2l+1) T_l, \quad (2)$$

where T_l is the transmission coefficient for a particle of angular momentum l . For proton capture the transmission coefficients were taken from the compilation of Feshbach *et al.*²⁰ for values of $Y \equiv \epsilon/B \leq 1.8$. In this compilation the nuclear potential is represented by a totally absorbing square well, and B is the Coulomb barrier height. An approximate form

$$\sigma_c = \pi(R+\lambda) \{ R[(Y-1)/Y] + \lambda \},$$

derived on the basis of a classical model¹⁹ which assumes that every particle striking the nucleus is captured, was used in the range $Y \geq 1.8$. The classical form was normalized to fit smoothly to the quantum-mechanical range $Y \leq 1.8$ and approach geometrical at $Y = \infty$. Two choices of the nuclear radius were used corresponding to $r_0 = 1.3$ and 1.5 F.

Subsequent to the time the present calculations were made, proton-reaction cross sections based on the more realistic optical-model potential have been calculated by Mani, Melkanoff, and Iori.²¹ A comparison of these cross sections with those calculated by Feshbach *et al.* for a totally absorbing square well has been reported by West.²² West has found that only slight changes in calculated proton spectral shapes at low energies result from the use of inverse cross sections fitted to the optical-model data of Mani *et al.* In view of this experience the use of σ_c based on optical-model transmission

coefficients would not be expected to alter appreciably the results of the present analysis.

Derivations of the level density based on the Fermi-gas model have been given by several authors. A typical approximate result is given by Ericson²³ in the form

$$\omega(E) = \frac{1}{12} (\pi^2/a)^{1/4} e^{2\sqrt{aE}} / (E)^{5/4}, \quad (3)$$

for free nucleons of both spins confined to move in a volume of radius $R = r_0 A^{1/3}$. The level-density parameter a is related to the single nucleon density g at the Fermi level through the relation $a = \pi^2 g/6$. In Eq. (3), $\omega(E)$ is the density of states at a given excitation energy, summed over all values of angular momentum J . The density of states at the excitation E of spin J is given in the same approximation by the relation

$$\omega(E, J) = \frac{(2J+1)}{2(2\pi)^{1/2} \sigma^3} \exp[-J(J+1)/2\sigma^2] \omega(E). \quad (4)$$

The above form has wide applicability since under many experimental conditions particles are emitted into residual states spanning a narrow range of spins. The parameter σ^2 is the mean square projection of the angular momentum J on a fixed axis and is sometimes called the spin cutoff parameter. The parameter σ^2 will in general be excitation energy-dependent.

If the Fermi-gas model is assumed the energy dependence of the level density may be represented by the general form

$$\omega(E) \propto E^{-n} e^{2\sqrt{aE}}, \quad (5)$$

where the choice $n = 5/4$ corresponds to Eq. (3) and $n = 2$ corresponds closely to Eq. (4) if allowance is made for the dependence of σ on E . The choice $n = 0$ approximates Eqs. (3) and (4) at high ($E > 5$ MeV) excitation energy. On the other hand, the level density takes the form

$$\omega(E) \propto e^{E/T}, \quad (6)$$

if a constant nuclear temperature $1/T \equiv d[\ln\omega(E)]/dE$ is assumed. The use of a constant temperature model is motivated largely by its simplicity and approximates the form of Eq. (3) or (4) at low (1–3 MeV) excitation energy.

A FORTRAN program was written for the IBM 709 computer which was used to reduce the data to a form in which the statistical model features were more easily extracted. The program uses as input data the number of counts per channel as a function of channel energy, energy calibration information including the possibility of target thickness, absorber, detector or electronic response nonlinearity corrections, and all entrance and exit channel information pertaining to center-of-mass transformations. The program computes for each channel the laboratory proton energy E_{lab} , the exit-channel energy, the excitation energy and the square root of the excitation energy. The program also computes the

¹⁹ J. M. Blatt and V. F. Weisskopf, *Theoretical Nuclear Physics* (John Wiley & Sons, Inc., New York, 1953).

²⁰ H. Feshbach, M. M. Shapiro, and V. F. Weisskopf, Nuclear Development of America Report No. 15B-5 (unpublished).

²¹ G. S. Mani, M. A. Melkanoff, and I. Iori, Commissariat à l'Énergie Atomique Report No. CEA-2379, 1963 (unpublished).

²² R. W. West, *Phys. Rev.* **141**, 1033 (1966).

²³ T. Ericson, *Advan. Phys.* **9**, 425 (1960).

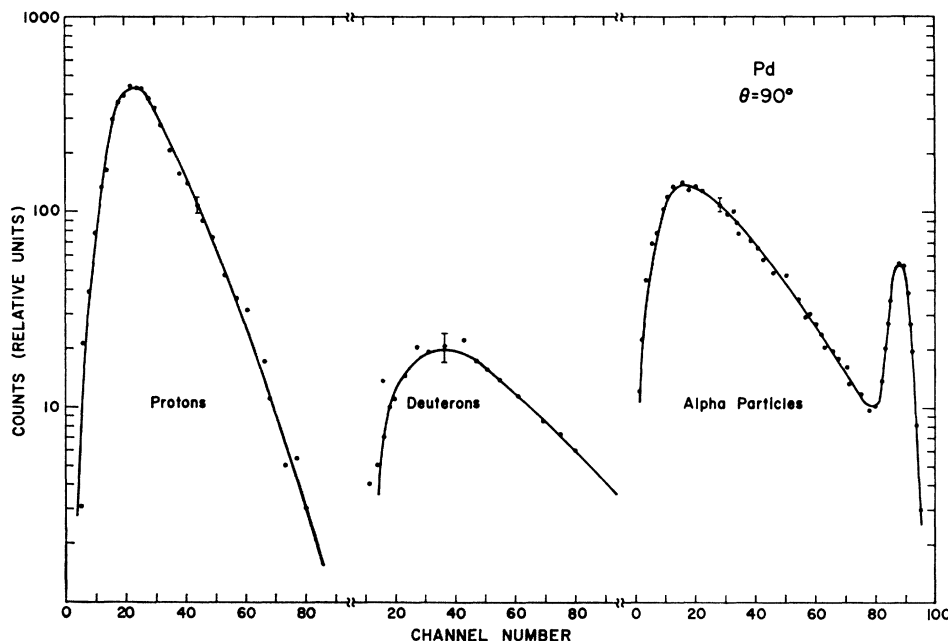


FIG. 4. The relative yields of protons, deuterons, and alpha particles at 90° in the laboratory induced by bombardment of Pd with 30.5-MeV alpha particles.

differential cross section $d^2\sigma/d\Omega dE$, $\ln d^2\sigma/d\Omega dE$, $\ln(d^2\sigma/d\Omega dE)/\epsilon\sigma_c$ and $\ln(d^2\sigma/d\Omega dE)E^2/\epsilon\sigma_c$ as a function of E_{lab} , E and \sqrt{E} .

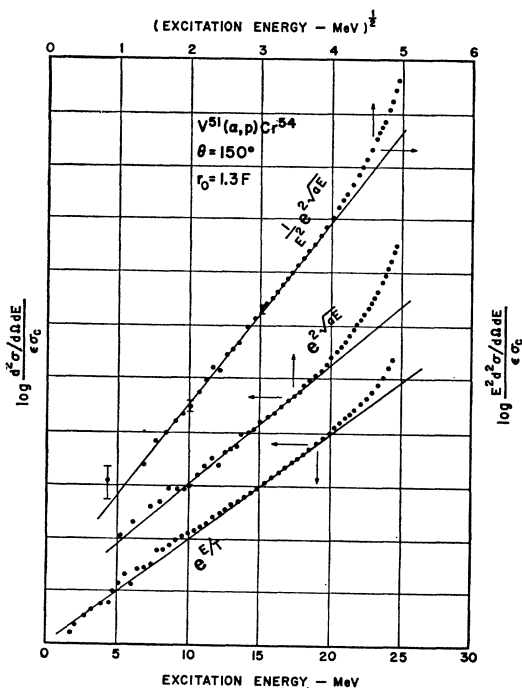


FIG. 5. The proton spectrum from the $V^{51}(\alpha, p)Cr^{54}$ reaction at 150° is represented in different forms appropriate to different level density prescriptions. The upper two curves correspond to different approximations of the Fermi-gas model and the lower curve to the constant-temperature approximation. The logarithms are to the base 10.

An example of the energy spectra accumulated in the memory of the 512-channel analyzer is shown in Fig. 4. It is seen that the emission of low-energy particles is strongly inhibited by the Coulomb barrier. At higher energies the spectra have an exponential shape characteristic of compound nuclear formation and subsequent evaporation. The elastic group is present in the highest channels of the alpha-particle spectra.

The experimental proton-emission spectrum for $V^{51}(\alpha, p)Cr^{54}$ at 100° is displayed in Fig. 5 in a manner such that the representations of the Fermi-gas model for $n=0$ and $n=2$ and the constant-temperature model may be compared. Either of these forms represents the data well up to an excitation energy of 15 to 20 MeV; however, it is evident that the two forms of the Fermi-gas representation lead to rather different values of the

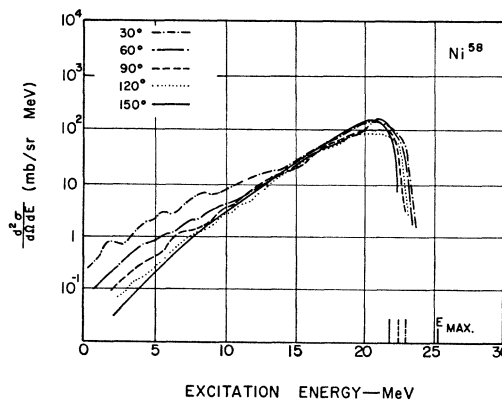


FIG. 6. $Ni^{58}(\alpha, p)Cu^{61}$; semilogarithmic plot of the differential cross section in mb/sr MeV as a function of excitation energy of the residual nucleus for five laboratory angles.

level-density parameter a . All subsequent analysis was made using the Fermi-gas form for the choice $n=2$.

4. RESULTS

The angular dependence of the cross section as a function of excitation energy is illustrated by the spectra of Figs. 6-13. The cases illustrated by these figures are representative of the angular dependence of the cross

section in each mass region. The curves in these figures were drawn smoothly through the data points. The cross section at low excitation energies shows a considerable amount of forward peaking. The forward peaking decreases with increasing excitation energy and mass number. Such features are common to direct reactions. At higher excitation energies (viz. 15-25 MeV for light and medium-weight elements and 5-18 MeV for heavy elements) the cross sections show no forward peaking and are either isotropic or symmetric about 90°. Such features are more characteristic of a compound-nuclear-

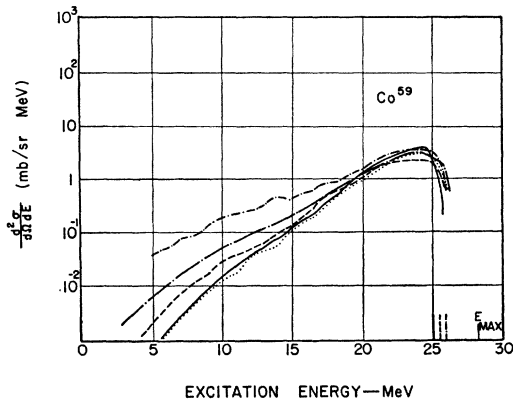


FIG. 7. $Co^{59}(\alpha, p)Ni^{62}$; see Fig. 6 caption.

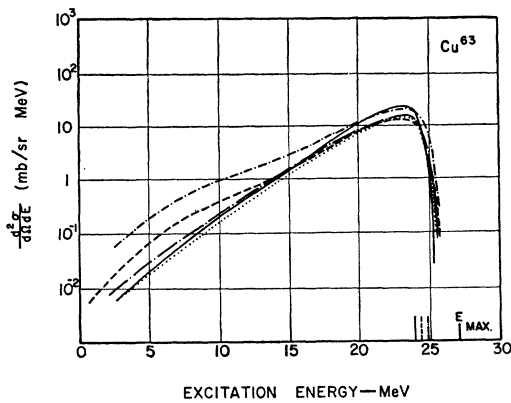


FIG. 8. $Cu^{63}(\alpha, p)Zn^{66}$; see Fig. 6 caption.

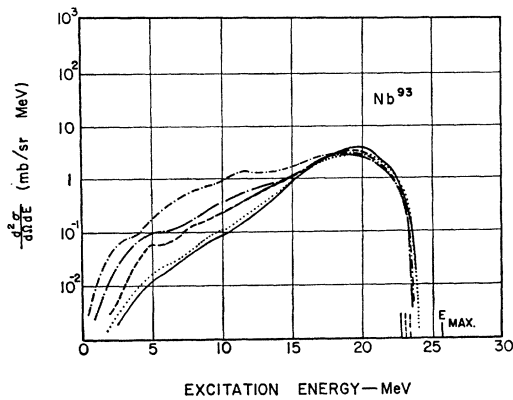


FIG. 9. $Nb^{93}(\alpha, p)Mo^{96}$; see Fig. 6 caption.

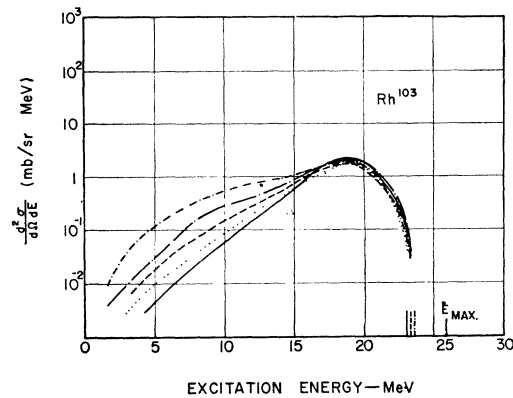


FIG. 10. $Rh^{103}(\alpha, p)Pd^{106}$; see Fig. 6 caption.

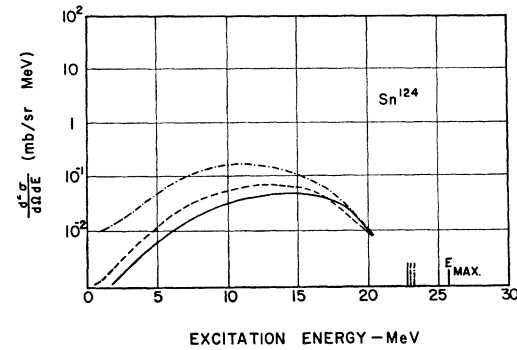


FIG. 11. $Sn^{124}(\alpha, p)Sb^{127}$; see Fig. 6 caption.

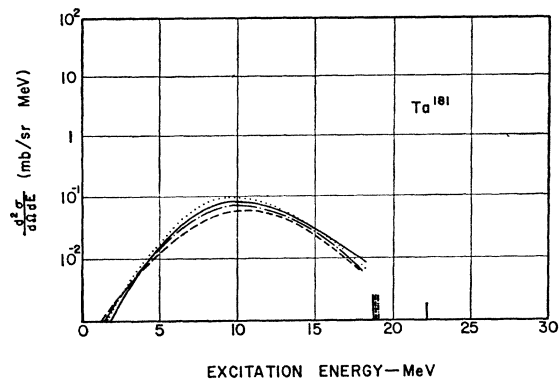


FIG. 12. $Ta^{181}(\alpha, p)W^{181}$; see Fig. 6 caption.

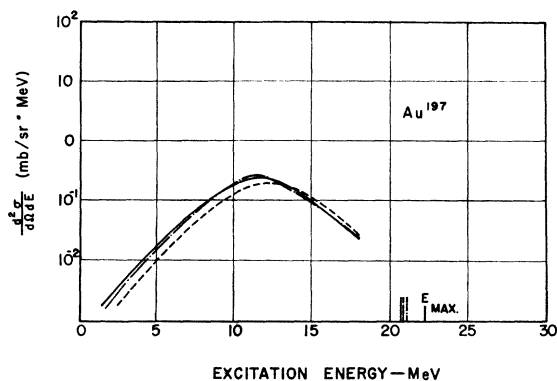


FIG. 13. $\text{Au}^{197}(\alpha, p)\text{Hg}^{200}$; see Fig. 6 caption.

reaction mechanism. The Coulomb barrier becomes prohibitive to charged-particle emission leading to states of the residual nucleus above 20 to 25 MeV. Low-energy protons below the 1.5-MeV detector and electronic threshold were not experimentally observed. The corresponding upper limit on the excitation energy is shown on the energy axis of Figs. 6-13 for each laboratory angle.

The ultimate success of the statistical analysis depends on the degree of completeness by which the

reaction mechanism may be described as proceeding through the compound nucleus. It is clear that compound-nucleus formation and decay is not the only mechanism involved in the (α, p) reaction initiated by 30.5-MeV alpha particles, since the statistical-model prediction of angular isotropy (or symmetry about 90° c.m.) of the reaction products is at variance with the experimental angular distributions at some excitation energies. Nevertheless, as has been pointed out, the angular distributions tend toward isotropy at the largest angles and such an angular dependence indicates that direct reactions play a minor role at these angles. The point of view is taken that the reaction mechanism at 150° is predominantly compound-nucleus formation and decay, and subsequent statistical-model analysis is made on this basis.

The problem of distinguishing between compound-nuclear and noncompound-nuclear events has also been considered recently by West²² using a different approach. In analyzing the proton spectra from reactions induced by 42-MeV alpha particles, West bases the identification of noncompound-nuclear events on the difference between the observed spectra and the calculated spectra for compound nuclear events. In such an approach level density parameters as predicted by statistical theory are used to generate the theoretical proton spectra. Hence,

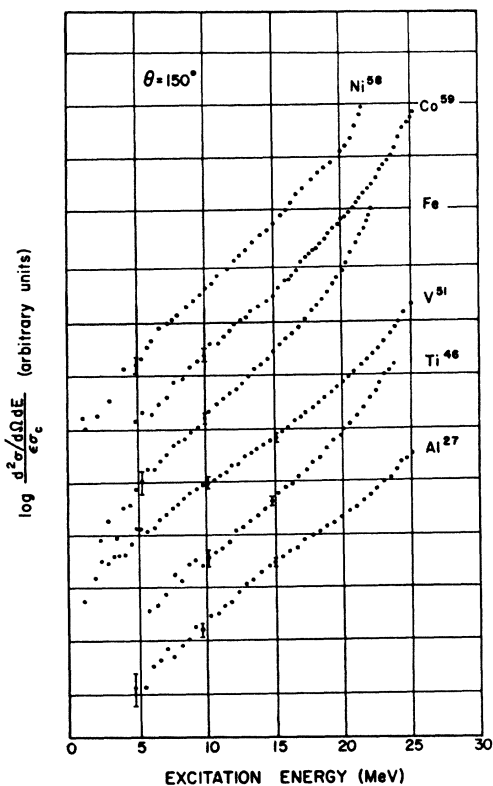


FIG. 14. The quantity $\log_{10}\{(d^2\sigma/d\Omega dE)/\epsilon\sigma_c\}$ for $\theta=150^\circ$ is represented as a function of excitation energy for the (α, p) reaction on targets of Al^{27} , Ti^{48} , V^{51} , Fe , Co^{59} , and Ni^{58} .

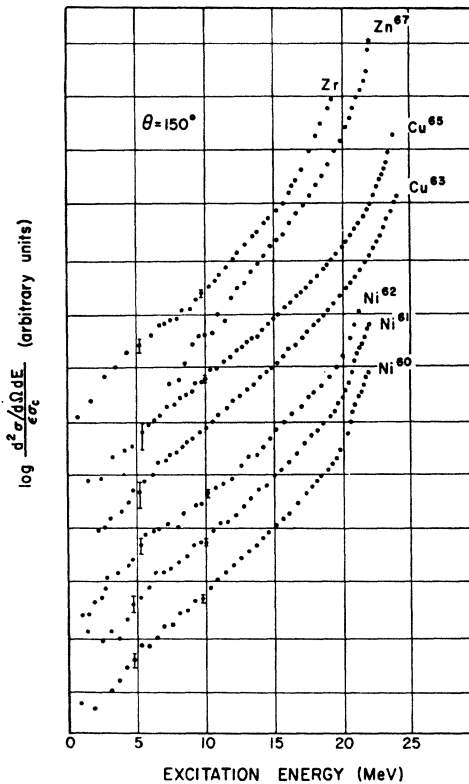


FIG. 15. The quantity $\log_{10}\{(d^2\sigma/d\Omega dE)/\epsilon\sigma_c\}$ for $\theta=150^\circ$ is represented as a function of excitation energy for the (α, p) reaction on targets of Ni^{60} , Ni^{61} , Ni^{62} , Cu^{63} , Cu^{65} , Zn^{67} , and Zr .

such an approach does not lead to an experimental determination of level density parameters but rather establishes a basis of estimating the fraction of the proton yield which is "statistical" in nature. West's analysis reveals that a significant fraction of the proton spectra from reactions induced by 42-MeV alpha particles is due to noncompound-nuclear events.

The quantity $\log_{10}\{(d^2\sigma/d\Omega dE)/\epsilon\sigma_c\}$ for the (α, p) reactions at 150° on 25 targets Al²⁷-Au¹⁹⁷ is represented in Figs. 14-17 as a function of the excitation energy of the residual nuclei. It is from the slopes of these plots that the nuclear temperature is extracted as defined by Eq. (6). The points in the figures are experimental and the errors indicated are statistical errors. The energy dependence is in general smooth and slowly varying at excitation energies ($E > 4$ MeV) where the continuum model is expected to be appropriate.

The quantity $\log_{10}\{(E^2 d^2\sigma/d\Omega dE)/\epsilon\sigma_c\}$ for the same reactions is shown in Figs. 18-21 as a function of the square root of the excitation energy of the residual nuclei. It is from the slopes of these plots that the level-density parameter a of the Fermi-gas model is determined as defined by Eq. (5) with $n=2$. The values of T and a so determined are tabulated in Table I. The parameters T and a were obtained from the linear sections of the plots which correspond to the excitation

energy range 2 to 3 MeV to around 20 MeV for the lightest targets and 2 to 3 MeV to about 15 MeV for the heaviest ones. The deviation of the plots in Figs. 14-21 from linearity above 20 MeV for lighter targets and above about 15 MeV for the heavier ones may be accounted for by the emission of protons as secondary emission products from such competing reactions as (α, np) , (α, pp) , and $(\alpha, \alpha p)$.

5. DISCUSSION

Values of the level-density parameter a obtained from the present experiment are compared in Fig. 22 (solid circles) with those obtained from other experiments involving alpha-particle-induced reactions. The parameter a is plotted as a function of the mass number of the residual nucleus. The first feature we note from the figure is that a is quite dependent upon the incident alpha-particle energy; those experiments performed with the highest incident energies yield the lowest values of a . The range of alpha-particle bombarding energies covered in these experiments extend from 9.6 to 40 MeV. The lowest a values reported are from the (α, p) experiment of Eisberg, Igo, and Wegner⁸ at 40-MeV incident energy, followed by those from the present experiment at 30.5 MeV. Lassen and Siderov⁹ in their (α, p) reaction study using 11.9- to 19.3-MeV alpha

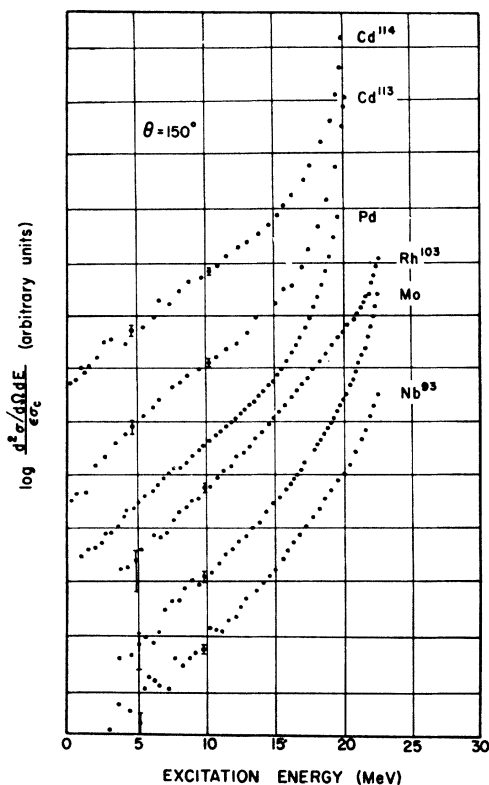


FIG. 16. The quantity $\log_{10}\{(d^2\sigma/d\Omega dE)/\epsilon\sigma_c\}$ for $\theta=150^\circ$ is represented as a function of excitation energy for the (α, p) reaction on targets of Nb⁹³, Mo, Rh¹⁰³, Pd, Cd¹¹³, and Cd¹¹⁴.

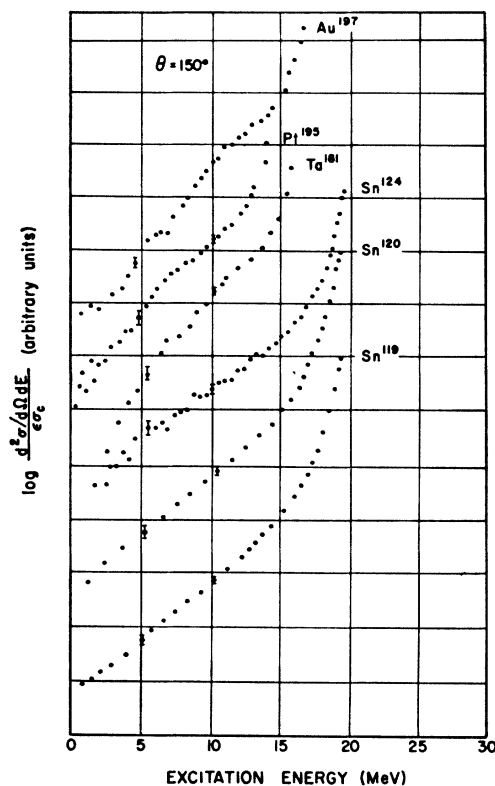


FIG. 17. The quantity $\log_{10}\{(d^2\sigma/d\Omega dE)/\epsilon\sigma_c\}$ for $\theta=150^\circ$ is represented as a function of excitation energy for the (α, p) reaction on targets of Sn¹¹⁸, Sn¹²⁰, Sn¹²⁴, Ta¹⁸¹, Pt¹⁹⁵, and Au¹⁹⁷.

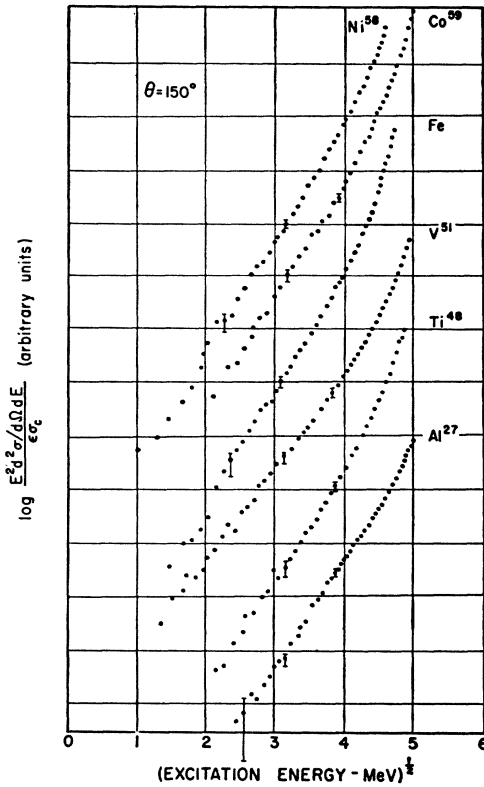


FIG. 18. The quantity $\log_{10}\{(E^2 d^2 \sigma / d\Omega dE) / \epsilon_c\}$ for $\theta = 150^\circ$ is represented as a function of the square root of the excitation energy for the (α, p) reaction on the targets Al^{27} , Ti^{48} , V^{51} , Fe , Co^{59} , and Ni^{58} .

TABLE I. Parameters from statistical analysis of 150° (α, p) data using $r_0 = 1.3 \text{ F}$.

Target	a (MeV^{-1})	T (MeV)
Al^{27}	5.4	2.15
Ti^{48}	5.6	1.78
V^{51}	4.9	2.12
Fe	5.0	1.68
Ni^{58}	6.7	1.58
Co^{59}	6.3	1.68
Ni^{60}	6.0	1.72
Ni^{61}	5.2	1.82
Ni^{62}	4.9	1.76
Cu^{63}	5.6	1.74
Cu^{65}	4.8	1.92
Zn^{67}	5.2	1.82
Zr	5.3	1.73
Nb^{93}	5.7	1.64
Mo	6.7	1.54
Rh^{103}	6.9	1.60
Pd	4.5	1.79
Cd^{113}	4.9	1.83
Sn^{119}	4.6	1.80
Sn^{120}	5.0	1.88
Sn^{124}	4.2	2.10
Ta^{181}	7.2	1.48
Pt^{195}	6.1	1.52
Au^{197}	7.2	1.41

particles found the parameter a at a fixed residual excitation energy to decrease strongly with increasing bombarding energy. The range over which a was found to vary in their experiment is shown by connected open squares in Fig. 22. The parameter a exhibited a similar energy dependence over the incident alpha particle energy range of 11.2 to 19.6 MeV in the (α, n) experiment of Siderov¹⁰ and is similarly represented in the figure. However, no energy dependence of a was observed in the (α, p) experiment of Fox and Albert.¹¹ The last-mentioned measurements were made at the lowest reported incident energies of 9.6 to 12.8 MeV. At 20 MeV incident alpha-particle energy (α, α') studies have been reported by Fulbright, Lassen, and Paulsen¹² and at the same energy (α, α') and (α, p) studies have been made by Hurwitz, Esterlund, and Pate.¹³

The solid curve of Fig. 22 represents the semi-empirical, shell-dependent level-density-parameter prediction of Newton⁴ as modified by Lang.² A second feature to be noted is the almost complete lack of agreement between the presently reported experimental points and Newton's theoretical curve. The disagreement is particularly noticeable for large mass numbers where experimental values of a are only about one third of the expected values. The Newton prediction of the mass dependence of a has been found to agree very well

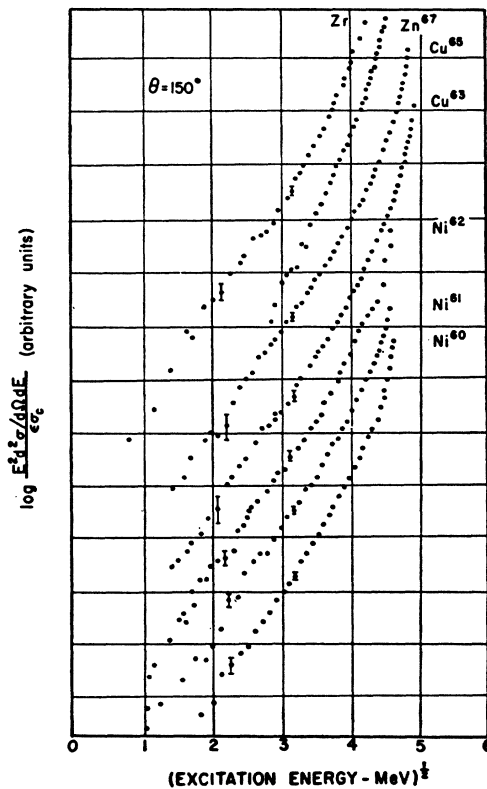


FIG. 19. The quantity $\log_{10}\{(E^2 d^2 \sigma / d\Omega dE) / \epsilon_c\}$ for $\theta = 150^\circ$ is represented as a function of the square root of the excitation energy for the (α, p) reaction on the targets Ni^{60} , Ni^{61} , Ni^{62} , Cu^{63} , Cu^{65} , Zn^{67} , and Zr .

with other classes of data. As was pointed out in the introduction comprehensive comparisons^{2,3} have been made between the Newton form of a and values derived from neutron- and proton-induced particle emission spectra and excitation functions as well as from direct level counting near neutron binding energy. Since such surveys have found the theoretical and experimental values to be in very good agreement, the disagreement here would seem to lie in the use of alpha particles as the incident particle or in the detailed application of the statistical model to the (α, p) , (α, n) , and (α, α') reactions.

Such features as the shape of the particle-emission spectra, angular distributions, and yields from the above mentioned alpha-particle-induced experiments are satisfactorily accounted for by the statistical model. The anomalous dependence of the level density parameter a , or the corresponding nuclear temperature, on the energy of the bombarding particle stands as a contradiction between present experimental observations and the predictions of the model. According to a straightforward interpretation of the statistical model, the same level-density parameters should be obtained when a reaction is studied at several incident energies, as long

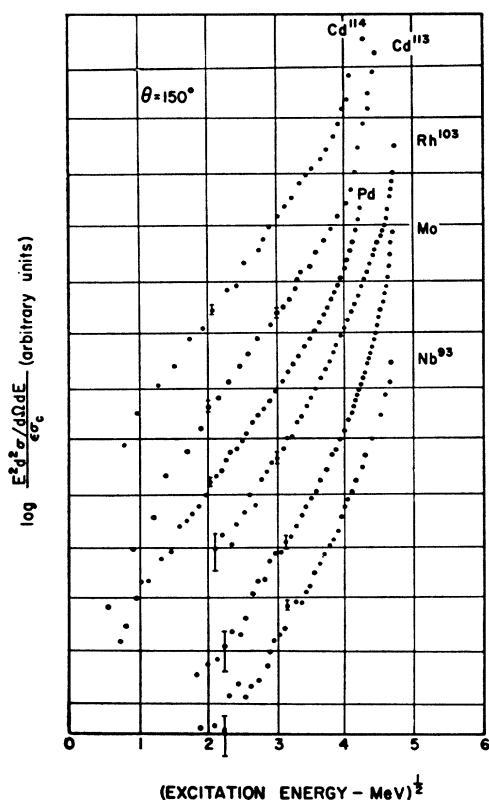


FIG. 20. The quantity $\log_{10}\{(E^2 d^2 \sigma / d\Omega dE) / \epsilon \sigma_e\}$ for $\theta = 150^\circ$ is represented as a function of the square root of the excitation energy for the (α, p) reaction on the targets Nb⁹³, Mo, Rh¹⁰³, Pd, Cd¹¹³, and Cd¹¹⁴.

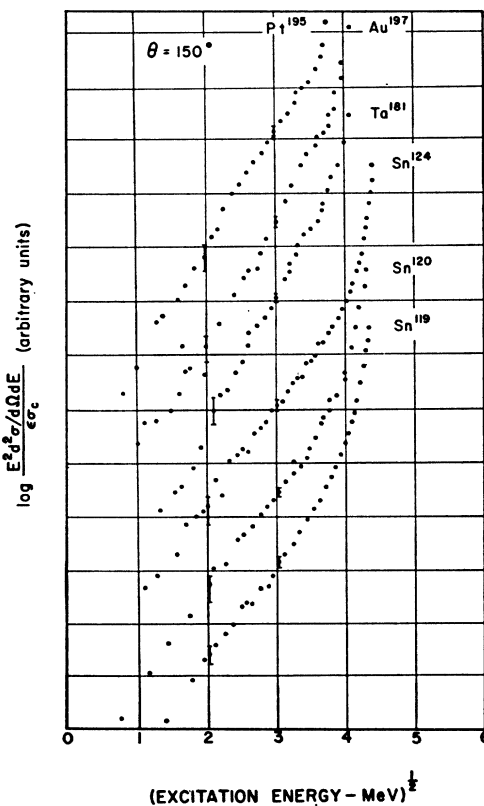


FIG. 21. The quantity $\log_{10}\{(E^2 d^2 \sigma / d\Omega dE) / \epsilon \sigma_e\}$ for $\theta = 150^\circ$ is represented as a function of the square root of the excitation energy for the (α, p) reaction on the targets Sn¹¹⁹, Sn¹²⁰, Sn¹²⁴, Ta¹⁸¹, Pt¹⁹⁵, and Au¹⁹⁷.

as the spectra are analyzed at the same residual excitation energy.

We shall next systematically consider a number of possible explanations for the "level-density-parameter anomaly." The presence of direct interactions has been most conspicuous in (p, p') spectra^{24,25} and to a lesser degree in (p, n) spectra. The direct-reaction contribution to particle-emission spectra is usually considered to manifest itself as a slowly falling tail at high emission energies. The presence of additional higher energy particles in the spectrum from direct reactions tends to flatten the emission spectrum decreasing the slope of plots like those in Figs. 18-21 and yielding lower a values. It has also been previously remarked that forward peaking of the angular distribution has been traditionally taken as evidence of a direct interaction contribution. However, the characteristic high-energy tail and forward peaking present in some (p, p') spectra are not present in the (α, p) data discussed here at the angles and excitation energies where the parameters are determined.

The yield from the direct-reaction process must be

²⁴ P. C. Gugelot, Phys. Rev. 93, 425 (1954).

²⁵ R. M. Eisberg and G. Igo, Phys. Rev. 93, 1039 (1954).

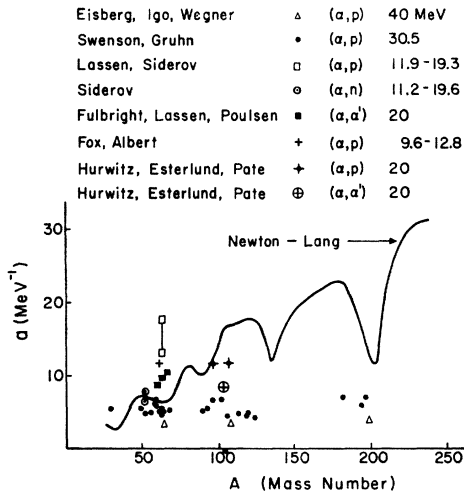


FIG. 22. Values of the level-density parameter a obtained from the present experiment are compared with those obtained from other experiments involving alpha-particle-induced reactions and with the prediction of Newton's shell-development formula as modified by Lang.

considered relative to the yield from statistical emission. Considering the isotopes of nickel from Ni^{58} to Ni^{62} , the relative importance of direct reactions should be greatest for Ni^{62} , for which the proton-emission probability is the lowest among the nickel isotopes. The measured level-density parameters for the nickel and copper isotopes in Table I reflect a possible limited role of direct interactions. However, the dependence of the level-density parameter on the incident alpha-particle energy was found by Lassen and Siderov⁹ to be the same for Cu^{63} and Cu^{65} , although the total proton yields differ by nearly a factor of 4. The influence of direct reactions seems very minor in the (α, p) reactions considered here and in any event could not be expected to account for the very large difference between the presently reported and the theoretically predicted a values.

The inverse capture cross section is a frequently mentioned possibility of the source of error in obtaining level-density parameters. The inverse capture cross section used in the present analysis involves simplifying assumptions regarding the nuclear surface. In the analysis of our data the barrier and consequently the form of $\sigma_c(\epsilon)$ was altered by using two different values of the radius, $r_0=1.3$ and 1.5 . The values were only slightly modified thereby. Lassen and Siderov⁹ who used substantially the same $\sigma_c(\epsilon)$ as used in the present analysis found that they could not account for the incident-energy dependence of the temperature by using different values of r_0 . The fact the incident-energy dependence persists in the (α, n) experiment of Siderov¹⁰ is further evidence that simplifying assumptions made regarding charged-particle barrier penetration are not responsible for observed anomalies in the (α, p) and (α, α') reactions. In general the approximations in-

involved in our assumed values of $\sigma_c(\epsilon)$ cannot account for the anomaly we are discussing, since $\sigma_c(\epsilon)$ does not vary sufficiently rapidly with ϵ in the relevant region.

Another possible explanation to be considered is the role played by the angular momentum of the compound nucleus at higher incident energies. As an aid to understanding the role played by the angular momentum of the compound nucleus on the subsequent particle emission and level-density parameter determination, we may speak of a rotational energy $E_r = J_c^2 \hbar^2 / 2I$, in analogy to a classical rotating system of moment of inertia I . Energy conservation with rotational energy accounted for would require us to express the total excitation energy of the compound nucleus as a sum $E = E_0 + E_r$, where E_0 is the excitation due to internal modes of excitation only. According to our model when states of high angular momentum are populated in the compound nucleus there will be correspondingly less energy available to be carried away by emitted particles as kinetic energy. Thus the particle emission spectrum will suffer from a depletion of high-energy particles resulting in a higher a -value determination.

We may consider energy conservation to be supplemented by angular momentum conservation and write $\mathbf{J}_c = \mathbf{I} + \mathbf{J} + \mathbf{S}$, where the compound nucleus is considered to be formed with angular momentum J_c and decays to a state of the residual nucleus of spin J by the emission of a particle of spin S and orbital angular momentum l . The assumption that the decay of the compound nucleus is independent of any restrictions arising from angular momentum conservation would imply that there are also no restrictions on the accessible values of l and j . Such limitations are generally imposed because the value of the spin of the residual nucleus is not arbitrary. The limitation of the spin J is represented by the spin cutoff parameter of Eq. (4) and available values of l are limited by penetrability considerations. The above discussion implies that the compound nucleus excited to a high spin state may be inhibited from decaying to a low-lying state of the residual nucleus because of the paucity of high spin states at low excitation energies. Emission of high-energy particles would thus be inhibited. In any event the inclusion of angular-momentum effects in the statistical emission process is to produce larger values of the level density parameter a with increasing incident energy, which is opposite to the observed trend.

Other explanations of the anomaly under discussion have been offered. As mentioned in Ref. 7, it has been suggested^{26,27} that due to the short mean free path of alpha particles^{28,29} in nuclear matter, the incident energy of the alpha particle is shared only locally with a

²⁶ G. Igo and H. E. Wegner, Phys. Rev. **102**, 1364 (1956).

²⁷ V. F. Weisskopf, Proc. Am. Acad. Arts Sci. **82**, 360 (1952-1953).

²⁸ G. Igo and R. Thaler, Phys. Rev. **106**, 126 (1957).

²⁹ W. W. Cheston and A. E. Glassgold, Phys. Rev. **106**, 1215 (1957).

small number of nucleons before emission occurs, giving rise to a local high temperature (low a value). Such a process has been referred to as "spot heating." If this approach were adopted, the temperature would be expected to show an increasing relationship with increasing incident particle energy and the equation of state, $E = aT^2 - T$, requires that the level-density parameter a show a decreasing relationship with increasing incident energy. Such a qualitative trend is shown by the data of Fig. 22.

Siderov¹⁰ attributes the dependence of the level-density parameter on incident energy to processes in which emission occurs before complete statistical equilibrium has been reached. Such a process is visualized as being intermediate between a direct interaction and complete compound-nucleus formation and decay. On the average, emission into the exit channel occurs before full statistical equilibrium has been reached, but after the incident nucleon has undergone a few collisions with other nucleons in the target nucleus. The emission spectra may then be expected to resemble those from complete compound-nuclear formation, with an absence of pronounced characteristics of direct reactions such as high-energy tails and forward-peaked angular distributions, but with energy distributions weighted by the presence of more high-energy particles.

In the mass region $M < 67$ of Fig. 22 the agreement between theoretical and measured level-density parameters may be considered satisfactory. It would appear that for lighter nuclei very nearly complete statistical equilibrium has been achieved before particle emission whereas for heavier nuclei, where more particles are involved, emission occurs more prematurely.

The partial-equilibrium model for nuclear reactions has been developed quantitatively by Izumo.^{14,15} In this model the target nucleons are divided into two groups; N inert-core nucleons and the extra-core, surface nucleons. It is assumed that only these surface nucleons interact strongly with the n nucleons of the incident projectile, while the inert-core remains in its ground state but produces an average potential for the incident nucleons. The excitation energy brought into the compound system is shared among the $K = A - N + n$ outer nucleons. The density of levels in such a system is considerably less than that of the usual compound nucleus and when the level density form of Eq. (5) (for $n=2$) is specialized for the partial-equilibrium model it takes the form

$$\omega(E) \propto \left(\frac{K}{A+n}\right)^2 \frac{1}{E^2} \exp\left\{2\left[a_0\left(\frac{A+n}{K}\right)^{3/2} E\right]^{1/2}\right\}. \quad (7)$$

The parameter

$$a_0 = 6.11 \times 10^{-4} K^2 \quad (8)$$

was assumed to be independent of A , to have a quadratic dependence on the quantity K and evaluated empirically in Ref. 14. The partial-equilibrium-model

level-density parameter, which we define by

$$a_1 \equiv a_0 \left(\frac{A+n}{K}\right)^{3/2} = 6.11 \times 10^{-4} (A+n)^{2/3} K^{4/3} \quad (9)$$

is compared with the results of the present experiment in Fig. 23. The points are experimental and the curves correspond to Eq. (9) for two choices of the outer nucleon number K . Although agreement between the data and the model prediction is not quantitative the comparison does support the previously stated view that proton evaporation is taking place before complete statistical equilibrium is established, with the excitation energy being shared between 60 to 80 nucleons prior to emission. The exact value of the outer nucleon number K obtained from Fig. 23 should be taken with caution since the exact K dependence of a_0 in Eq. (8) has not been established. In general low level-density parameters which vary only slowly with mass number may be expected from the partial equilibrium model in contrast to usual statistical treatments.^{23,4}

At low incident energies the compound nucleus is usually formed as the end product of the compound system, whereas at high energies direct reactions involving only one target nucleon become likely. Thus it may be expected that the excitation energy brought into the system by the incident particle is shared among a smaller number of nucleons in the target nucleus as the incident energy increases. It is to be noted from Fig. 23 that for a given mass number A , lower values of the level density parameter are associated with smaller outer nucleon numbers. Such a behavior is consistent with the previously noted decreasing dependence on a on increasing incident energy.

The eigenstates of the partial equilibrium model are the intermediate resonance energies. The model predicts that intermediate resonances should appear commonly in all types of nuclear reactions in the medium excitation-energy region and that they should show

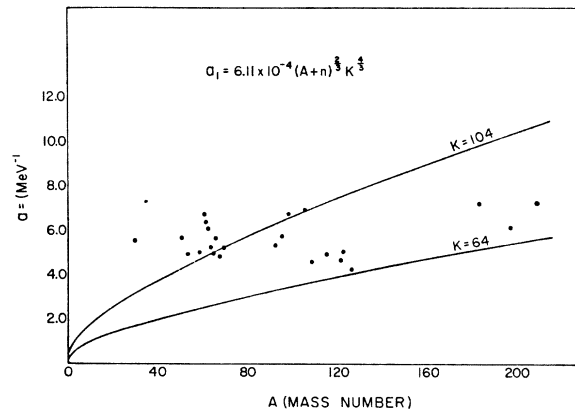


FIG. 23. The level-density parameter a , predicted by the Fermi-gas model as modified by the assumptions of the partial-equilibrium model of Izumo, is compared with the experimental values from the 30.5-MeV (α, p) experiment.

little of individual nuclear characteristics. A small fixed number of outer nucleons is responsible for the intermediate resonances, thus resonance parameters such as the total width Γ , of the order of 100 keV, should show little dependence on mass number. At the excitation energies reached in the present experiment even the widths of these broadly spaced states of the compound system will become greater than the level spacings implied by Eq. (7). At these excitation energies the presence of intermediate resonances may be seen, and their widths obtained, indirectly through the nuclear temperature or level density parameter. A statistical model expression for Γ has been given by Weisskopf³⁰ in the form

$$\Gamma = \frac{2gM}{\hbar^3\pi^2} \int_0^{\epsilon_{\max}} \frac{\sigma_c \epsilon \omega(E) d\epsilon}{\omega_c(U)}, \quad (10)$$

where g is a statistical weight factor, σ_c the inverse captive cross section, and M the reduced mass of the exit channel. The excitation energy of the compound nucleus U and the residual nucleus E are related by $E = \epsilon_{\max} - \epsilon$ and $\epsilon_{\max} = U - B$, and B is the binding energy in the compound nucleus of the emitted particle. The level density of the compound nucleus $\omega_c(U)$ and the residual nucleus $\omega(E)$ of Eq. (10) are usually assumed to have the same form which for ease of calculation we take to be $e^{E/T}$. After integrating Eq. (10) over the channel energy ϵ , assuming σ_c energy-independent, we obtain the approximate expression (for $\epsilon_{\max}/T \gg 1$)

$$\Gamma = \frac{Mg}{\hbar^3\pi^2} \sigma_c T^2 e^{-B/T}, \quad (11)$$

relating the width Γ to the nuclear temperature T . In Eq. (11), Γ decreases with decreasing temperature. Statistical treatments of the level-density parameter a ^{23,4} predict and increase in a from 3 to 21 over the range of mass values Al to Pb. The corresponding change in the temperature is a decrease from 1.8 to 0.65 over the same mass range if T and a are related through the equation of state

$$E = aT^2 - T, \quad (12)$$

at an average excitation energy of 8 to 9 MeV. For such a change of temperature Eq. (11) requires a change in Γ of a factor of 4×10^3 if $B = 6$ MeV. That is, if a value of $\Gamma_{Al} \simeq 18$ keV is assumed for aluminum^{31,32} at medium excitation energy, the statistical-model projection for a

nucleus in the lead region would be $\Gamma_{Pb} \simeq 4$ eV. Dearnaley *et al.*³² have obtained a coherence energy of $\Gamma_{Al} = 18$ keV from a statistical fluctuation analysis of the $Al^{27}(\alpha, p)$ reaction at an excitation energy of 17 MeV. Using Eqs. (11) and (12) the corresponding width at an excitation energy of 40 MeV, reached in the compound system of the present experiment, is estimated to be 195 keV for the same nucleus.

From the experimental data of Table I the temperature decreases by only the small amount of 1.8 to 1.5 over the aluminum-to-lead mass range and the required change of Γ from Eq. (11) is only a factor of 2.8. The measured temperatures are then consistent with a width Γ of the order of 18 keV at 10- to 20-MeV excitation over a wide range of mass numbers, if the compound system is assumed to reach complete statistical equilibrium for the (α, p) reaction in the aluminum region. Thus the unusually low and mass-independent characteristics of the measured a values may be a result of the role played by intermediate resonances as predicted by the partial-equilibrium model^{14,15} and the doorway-state model.^{16,17}

We do not imply that the intermediate resonances responsible for low a values in the (α, p) reaction are as specialized as the "doorway states," which are two-particle one-hole states, but rather arise from a more general system which may involve a larger number of particles. The states of this compound system have been called "hallway states" since they are intermediate in complexity between the three-quasiparticle doorway states and the much more complex compound nuclear configurations. Indeed, the concept of premature evaporation or partial equilibrium as it is used here involved a system of particles the number which may not be constant in every interaction, but the average of which is significantly less than A for medium-weight and heavy nuclei. The states of this system may be expected to have widths intermediate between those expected for doorway states (~ 100 to 200 keV) and the narrow compound-nuclear widths.

ACKNOWLEDGMENTS

The authors gratefully acknowledge the assistance of E. F. White and other members of the cyclotron operating crew who maintained the machine during the experimental phase of the study, and the assistance of Miss Betty Campbell with the computer programing. It is also a pleasure to acknowledge many helpful discussions with Dr. N. S. Wall and Dr. K. Izumo. Appreciation is also extended to Dr. D. W. Lang for discussions of his intermediate-resonance calculations prior to publication. The use of the MIT computation center is also appreciatively acknowledged.

³⁰ V. Weisskopf, Phys. Rev. 52, 295 (1937).

³¹ E. Gadioli, G. M. Marazzan, and G. Pappalardo, Phys. Letters 11, 130 (1964).

³² G. Dearnaley, W. R. Gibbs, R. B. Leachman, and P. C. Rogers, Phys. Rev. 139, 1170 (1965).